This is the accepted version of the manuscript. For the online version, please visit: https://doi.org/ 10.1109/JMEMS.2017.2654126

Reusable High Aspect Ratio 3D Nickel Shadow Mask

M.M.H. Shandhi[1], M. Leber[1], A. Hogan[2], D.J. Warren[3], R. Bhandari[2] and S. Negi[1,2]
[1]Department of Electrical and Computer Engineering, University of Utah, Salt Lake City, UT, USA
[2]Blackrock Microsystems, Salt Lake City, UT, USA
[3]Department of Bioengineering, University of Utah, Salt Lake City, UT, USA

Abstract—**Shadow Mask technology has been used over the years for resistless patterning and to pattern on unconventional surfaces, fragile substrate and biomaterial. In this work, we are presenting a novel method to fabricate high aspect ratio (15:1) three-dimensional (3D) Nickel (Ni) shadow mask with vertical pattern length and width of 1.2 mm and 40 µm respectively. The Ni shadow mask is 1.5 mm tall and 100 µm wide at the base. The aspect ratio of the shadow mask is 15. Ni shadow mask is mechanically robust and hence easy to handle. It is also reusable and used to pattern the sidewalls of unconventional and complex 3D geometries such as microneedles or neural electrodes (such as the Utah array). The standard Utah array has 100 active sites at the tip of the shaft. Using the proposed high aspect ratio Ni shadow mask, the Utah array can accommodate 300 active sites, 200 of which will be along and around the shaft. The robust Ni shadow mask is fabricated using laser patterning and electroplating techniques. The use of Ni 3D shadow mask will lower the fabrication cost, complexity and time for patterning out-of-plane structures.**

Index Terms—**3D Shadow Mask, Stencil, High Aspect Ratio, Microneedle, Neural Electrodes.**

I. INTRODUCTION

With the advent of micromachining various methods such as electron beam (e-beam) lithography, and deep-UV lithography have been used to pattern thin films on a substrate. Optical lithography has its limitations in patterning on out of plane substrate, organic material, fragile devices, plastics and biomaterials like proteins and cells. Laser patterning, focused ion beam (FIB) and different methods of 3D lithography, e.g., imprint lithography, holographic lithography, LIGA have demonstrated their application in patterning on high aspect ratio 3D structures [1]. One useful application of these techniques is in an array of microneedles and neural array such as the Utah Electrode Array (UEA), shown in figure 1. The UEA is widely used in neural prosthesis, which consists of 100 highly doped silicon microneedles [2]. The UEA consists of a ten by ten square grid of 1.5 mm long microneedle with 400 µm spacing between them. One hundred Pt/TiW/Pt bond pads are deposited on the back surface of these arrays, and one hundred 30 µm insulated gold wires are bonded to these pads and to a percutaneous connector for electrical connection to external electronics. The tip of each microneedle is metalized with platinum or iridium oxide to facilitate electronic to ionic charge transduction into the targeted tissue. The entire array, with the exception of the tip of each microneedle, is insulated with a biocompatible material, Parylene-C.

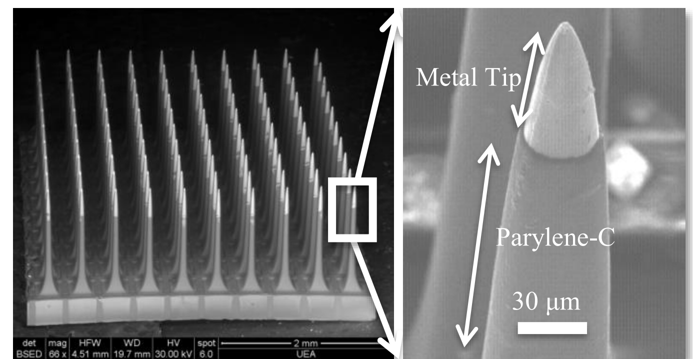

Fig 1. (Left) Scanning electron micrograph (SEM) of the 100 channel Utah Electrode Array (UEA), (Right) inset shows zoom-in view of the tip of the microneedle illustrating the active site [3].

The UEA is a gold standard neural device for the recording and stimulation of neural tissue. However, the UEA has a major limitation of having only one recording site per microneedle. Due to the complex three dimensional structure of the UEA it is not easy to have more than one recording site per microneedle. In our previous work [3], we have presented a device, the Utah Multisite Electrode Array (UMEA), which

Research reported in this publication was supported by the National Institute of Neurological Disorders and Stroke of the National Institutes of Health under Award Number R01NS085213. The content is solely the responsibility of the authors and does not necessarily represent the official views of the National Institutes of Health.

M.M.H. Shandhi was with the University of Utah, UT 84112 USA. He is now with Georgia Institute of Technology. GA, USA (e-mail: mobashir.shandhi@gatech.edu).

M. Leber is with the University of Utah, UT, 84112 USA. (e-mail: moritz.leber@utah.edu).

A. Hogan is with Blackrock Microsystems, UT 84108 USA (e-mail: ahogan@blackrockmicro.com).

D.J. Warren is with the University of Utah, UT, 84112 USA. (e-mail: david.warren@utah.edu).

R. Bhandari is with Blackrock Microsystems, UT 84108 USA (e-mail: rbhandari@blackrockmicro.com).

S. Negi is with Blackrock Microsystems, UT 84108 USA (e-mail: snegi@blackrockmicro.com).

has recording sites along and around the microneedle, making it a 3D neural array. It was envisioned that the proposed device will have 300 channels in the same foot print of the standard UEA with 100 channels. Research has been carried out to stack planar neural probes to achieve 3D assembly with channel counts between 64 and 100 [4-8]. The planar probe such as Michigan array is fabricated by standard lithography technology, whereas the UMEA, with its inherent out of plane structure, is fabricated using unconventional fabrication techniques. These planar neural electrode arrays have another limitation of having recording sites on one side of the shaft. The UMEA can have recording sites along and around the shaft. Hence, the UMEA will be able to record from the neuron which is behind the electrode unlike other planar electrodes. Furthermore, the planar probes were using inconvenient, tedious and unreliable stacking techniques to assemble with external circuitry which requires additional packaging steps.

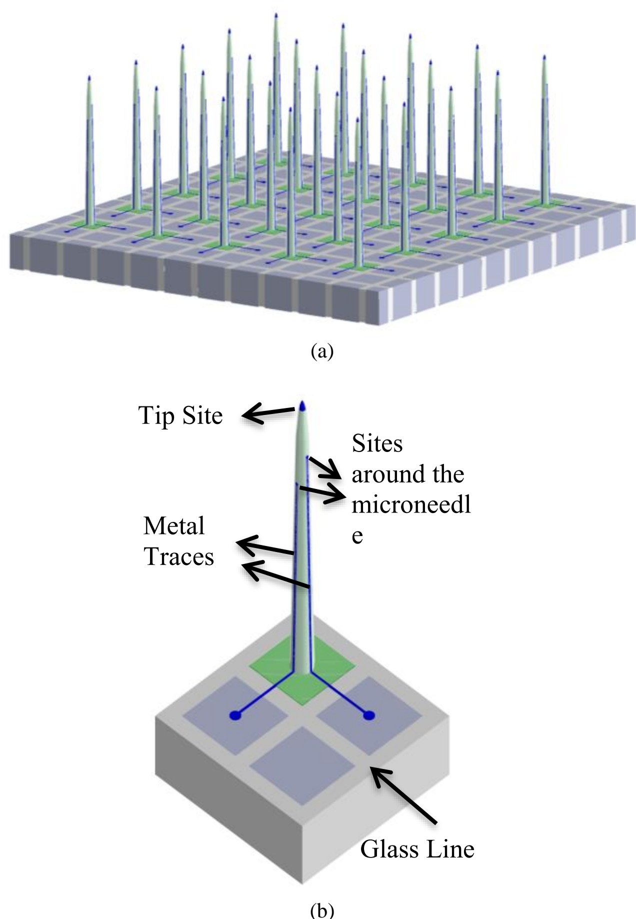

Figure 2: Schematics of the Utah Multisite Electrode Array (UMEA) with 3 active sites per microneedle: (a) isometric view of the device, (b) single microneedle with sites and metal traces coming down from the microneedle towards the base block.

The UMEA has the same configuration and form factor as that of the UEA. The base area around one microneedle is divided into electrically isolated blocks using glass layer; the microneedle occupies one block. Each base block has individual bond pads connected to them at the backside. The UMEA device, used in this work, has 3 active sites per microneedle; one active site at the tip and two others along the microneedle, 300 μm and 450 μm below the tip, as shown in figure 2. Individual metal traces run down from the sites to the isolated base areas. This array is coated with alumina and silicon nitride layer underneath the metal to electrically isolate the active sites and metal traces. The tip is connected to underneath bond pad through highly doped silicon substrate. Remaining sites are connected through isolated base blocks. Finally, the UMEA is coated with biocompatible polymer, Parylene-C and laser is used to remove Parylene-C from active sites. The UMEA is connected to a standard connector using wirebonding.

Previously, we used laser and FIB to create isolated sites and traces along the microneedle of the UMEA [3]. Choi et al. also used Excimer laser to facilitate electrodeposition of metal lines on highly inclined surface for application in 3D multi-electrode array [9]. Laser patterning and FIB are not parallel process and are not suitable for wafer scale fabrication. They showed operator dependent variability in the patterned layer and channel impedances for the UMEA devices. As an alternative, a process with more control such as shadow masking approach is presented in this paper.

Stencil lithography [10] and imprint lithography [11] have showed their application in overcoming drawbacks of optical lithography and laser pattering. We are using shadow mask for metal deposition on the UMEA devices to address variability and operator dependency.

Micro and nanostencil lithography have been used to pattern non-conventional substrates and biomaterials, due to its advantage of: (a) no resist processing, (b) easy manipulation and implementation, (c) reusability and (d) dynamic stencil lithography [10]. Stencils have been used in micromachining from long ago. Alix et al. first described the use of stencil to pattern glass [12] and Ingle et al. showed the use of stencil masks with sputtering thin films [13]. Dunkleberger also described the use of polymer/metal stencils for thin film Josephson devices [14] and Nguyen proposed the use of shadow mask for a more efficient deposition of metal contacts on solar cells, avoiding photoresist processing [15]. Burger et al. demonstrated the deposition of 3 μm wide features on non-planar substrates using stencils by shadow effect from planar mask [16]. Shadow masks have been used also to pattern on fragile MEMS structure [17] and non-planar surfaces where resist coating is difficult or impossible [18].

Brugger et al. used 3D shadow mask to define an array of metal wiring across a large topographical step [19]. The aspect ratio of pattern was approximately 5 with step height of 120 μm and width of 25 μm. Villanueva et al. explored the use of planar shadow mask to etch sloped walls [20]. Kang et al. used slanted deposition through shadow mask to deposit electrodes on vertical side wall [21]. Choi et al. used inclined UV lithography and 3-D metal transfer micromolding using planar shadow mask to pattern on microneedle sides [22]. In another work Jin Ho Choi et al. fabricated flexible stencil of PDMS and used that for patterned metal deposition on cylindrical surface [23]. They fabricated a planar shadow mask and attached the mask on cylindrical surface for deposition.

Fabrication of shadow mask has been done in various ways, like photolithography, stamping, micromolding and by using a release layer. All these technologies have their drawbacks for high aspect ratio structures like microneedles. In this work, we are presenting a novel fabrication technology for making high aspect ratio (15:1) Ni shadow mask, which is useful for complex and dense 3D geometries like the UMEA. The vertical pattern length and width achieved in this work are 1.2 mm and 40 µm respectively, i.e. pattern aspect ratio of 30:1. To the knowledge of the authors, no research has been reported on such high aspect ratio 3D shadow masks for microneedles. This nickel shadow mask is mechanically robust and reusable. It has its application in thin film processing to be used as a mask in 3D lithography, ion implantation and etching. Thin film metal deposition using this 3D shadow mask, on the UMEA device, is validated in this work.

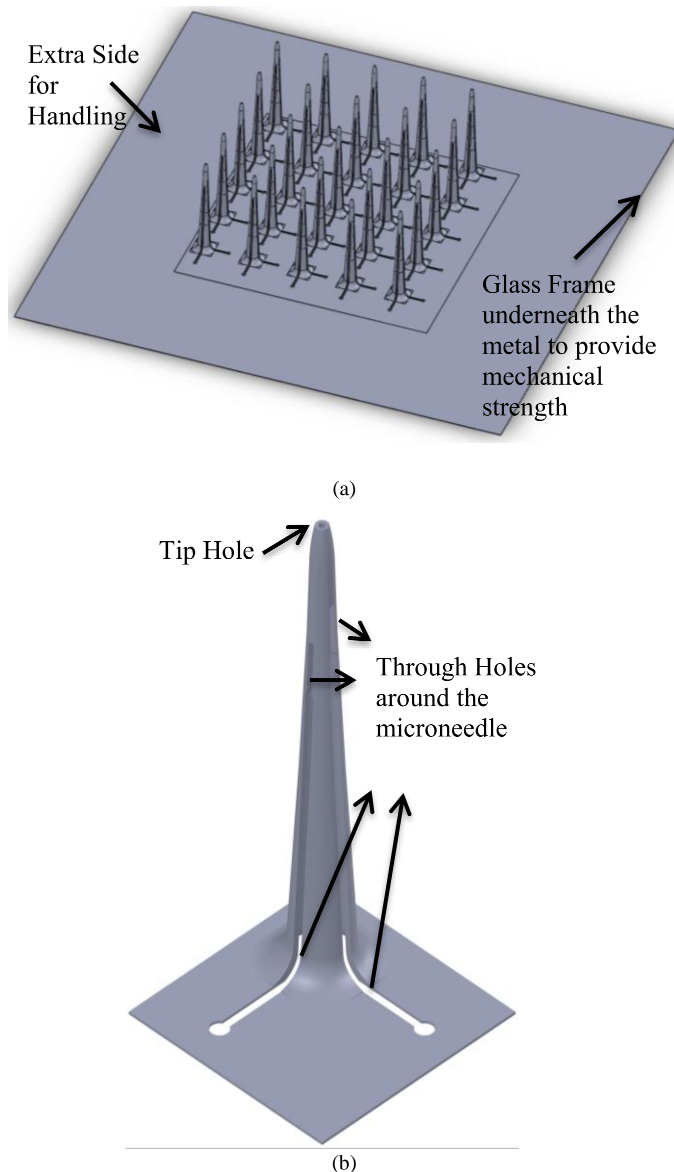

Figure 3: Schematics of shadow mask: (a) isometric view of the mask with extra side along the base for easy handling, (b) zoom in view of one microneedle in the mask with tip hole and channels coming down form the microneedle to the base.

II. Design

For the design and structure of shadow mask, a design similar to that of 5x5 UEA is chosen. It has a thickness of 25 µm and consists of 25 hollow microneedles with patterns across the needles towards the base, as shown in figure 3. Center to center distance between the hollow microneedles is 800 µm. The height of each hollow microneedle is 1.5 mm with a base width of 100 µm (i.e. aspect ratio of 15:1). Patterns/openings on shadow mask are chosen to have all the metal patterning on the UMEA device as shown in figure 2.

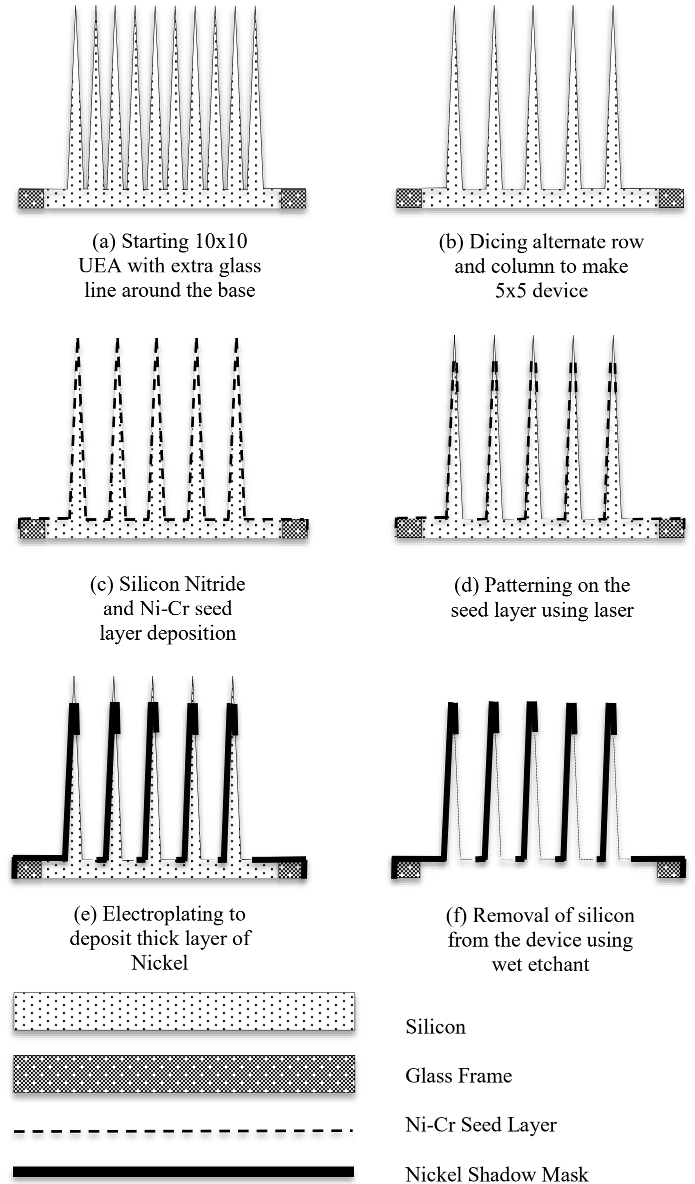

Figure 4: Fabrication steps of shadow mask: (a) starting 10x10 device with extra silicon and glass frame around the base, (b) dicing into 5x5 device, (c) deposition of insulation layer and seed layer, (d) laser pattering on seed layer, (e) electroplating in Nickel solution and (f) etching of silicon from underneath the metal.

Each hollow microneedle has patterned hole at the tip and two channels running from the tip to the base. The tip hole has a diameter of 50 µm. First channel starts from 300 µm below the tip and second one 150 µm below that. The two channels

are on orthogonal plane on the microneedle, with pattern width of 40 µm. Extra sides around the mask are used to assist handling. It has 800 µm wide glass frame underneath the metal, which helps the mask to be mechanically stable and prevents any bending in the structure.

III. Fabrication Methodology

Figure 4 depicts schematic view of the fabrication process flow. It starts with a 10x10 UEA (i.e. 400 µm pitch between the 1.5 mm long microneedle) without any backside metallic bond pad and any glass line between the microneedle bases. It has extra silicon all around the base with 800 µm wide glass frame. Figure 5(a) shows the starting device.

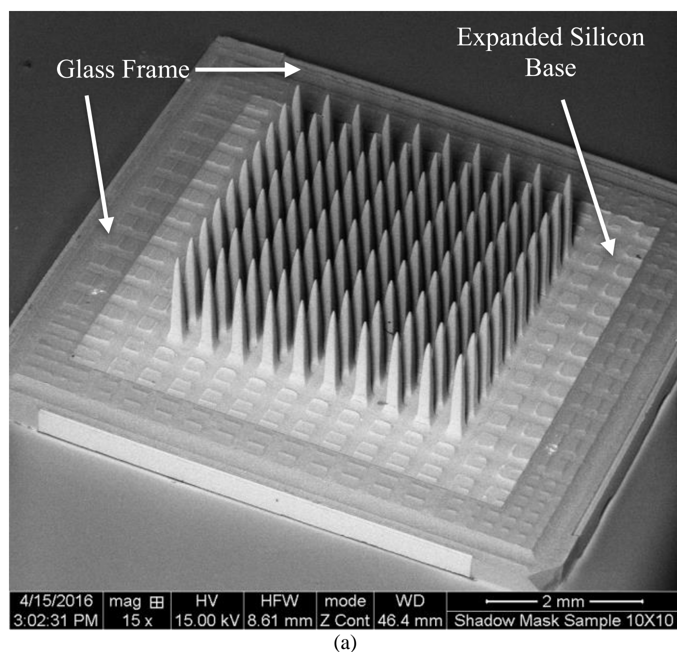

(a)

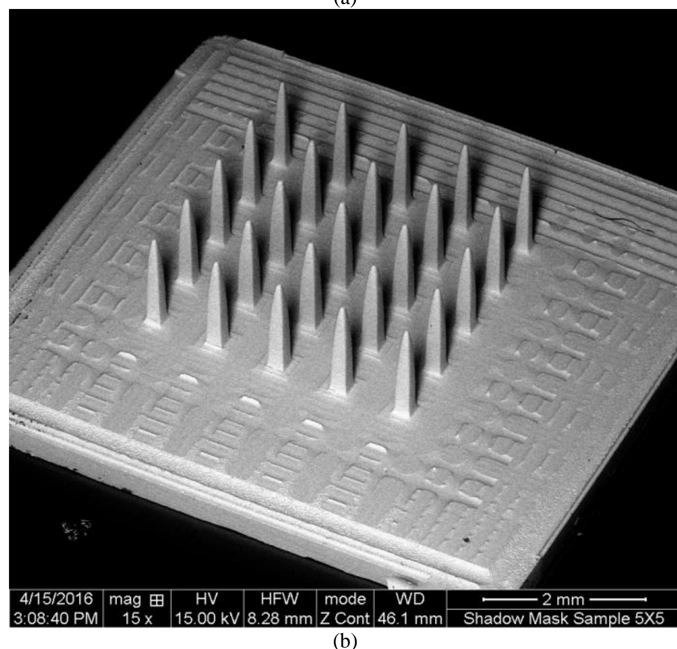

(b)

Figure 5: SEM of: (a) 10X10 UEA with extra silicon and glass frame around the base. (b) 5X5 sample after dicing, insulation layer and seed layer deposition

Fabrication methods started from dicing the device to remove alternate rows and columns and to make the device 5x5. Insulation (Silicon Nitride) layer was deposited on the device and then seed layer was sputtered. Laser was used to pattern the seed layer to make traces along the microneedle towards the base bond pad, i.e., seed layer was removed from the traces and insulation layer was exposed. The sample was electroplated to deposit thick metal layer to increase stability and reusability. Exposed insulation layer prevented the metal deposition in the patterns. Silicon was etched away thoroughly from the sample, from the backside and through the patterns using wet etchant solution. Sample was taken out of the solution and rinsed with water. Each of the manufacturing steps is explained in more details below.

A. *Dicing*

Disco dicing saw 3220, with 200 µm thick thermocarbon blade, was used to cut the alternate rows and columns from the 10x10 device to make it a 5x5 device. It involves 3 cuts with 100 µm pitch to remove one microneedle and after 3 cuts dicing saw was moved 600 µm to skip one row and start cutting next row of microneedle. Total 15 cuts were made from one direction to remove 5 rows of microneedle and the device was rotated by 90 degrees. Then another 15 cuts were made. The orthogonal 30 (15 from each direction) cuts removed total 75 microneedles and made the device 5x5 with 800 µm pitch between the microneedle. Figure 5(b) shows a 5x5 device. The device was then ultrasonically cleaned in acetone, isopropyl alcohol (IPA) and deionized (DI) water to remove all the dicing dusts.

B. Silicon Nitride Layer Deposition

Plasma-enhanced chemical vapor deposition (PECVD) was used to deposit 2 µm thick silicon nitride layer on the device to have an insulating layer underneath the seed layer. The deposition rate of silicon nitride was 25 nm per minute. We used Oxford Plasmalab 80 PECVD machine with N_2 flowing at 380 sccm, NH_3 flowing at 20 sccm and SiH_4 flowing at 20 sccm. Substrate temperature was 300°C and deposition pressure was 1 Torr. We ran the deposition process for 80 minutes and measured the thickness of silicon nitride using film thickness analyzer (Nanospec 3000). The thickness was 1.89 µm.

C. Seed layer Deposition

Seed layer, consisting of 50 nm Cr and 100 nm Ni, was sputter deposited on top of the device using Denton Discovery 18. Cr was deposited for 5 min for a deposition rate of 10 nm per minute, with 9.5 mTorr of pressure, 50 W of power and argon gas flow of 100 sccm. For Ni, 9.5 mTorr of pressure, 50 W of power, and argon gas flow of 100 sccm was used. Ni was sputtered for 10 minutes with a deposition rate of 10 nm per minute. We used Profilometer (Tencor P-10) to measure the thickness of the metal. The thickness of the metal was 147 nm.

D. Patterning on Seed layer

Laser was used to pattern the seed layer on the device, as per the schematic shown in figure 3. Excimer laser (Optec MicroMaster) with wavelength of 248 nm was used for

patterning. Seed layer was removed from the tip via focusing a demagnified laser spot with laser pulses of 5 ns in duration, with a repetition rate of 50 Hz. Spot size of 50 µm (diameter) with laser fluence of 967 mj/cm^2 was used for the tip.

For the through holes and patterns along the microneedle towards the base, sample was tilted by an angle of 20^0 to have access on the vertical microneedle. Continuous laser pulse with 50 µm per second scan speed, 50 Hz repetition rate and 50 µm spot size was used. After every 100 µm pass along the microneedle, focus was readjusted to make sure sample was in focus. Laser passes were carried out to completely remove the seed layer from the patterns and expose the silicon nitride layer underneath. Same parameters were used to complete the patterns on the base. Figure 6 shows the sample after seed layer pattering.

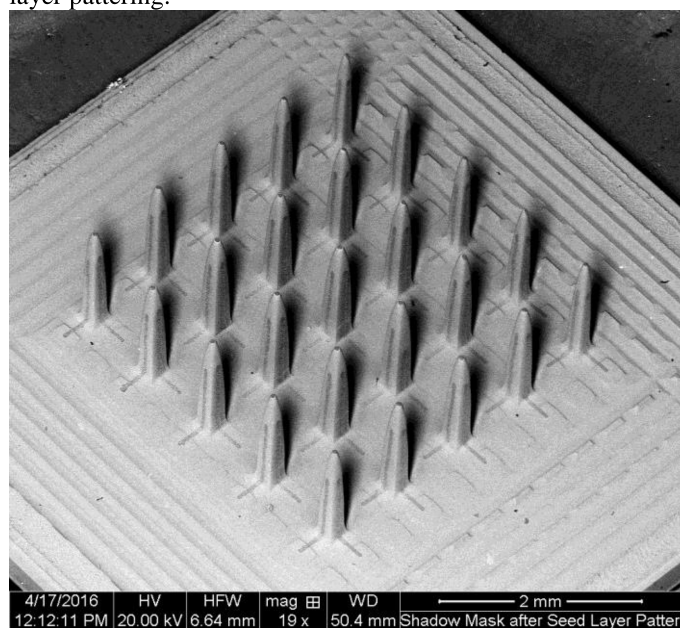

(a)

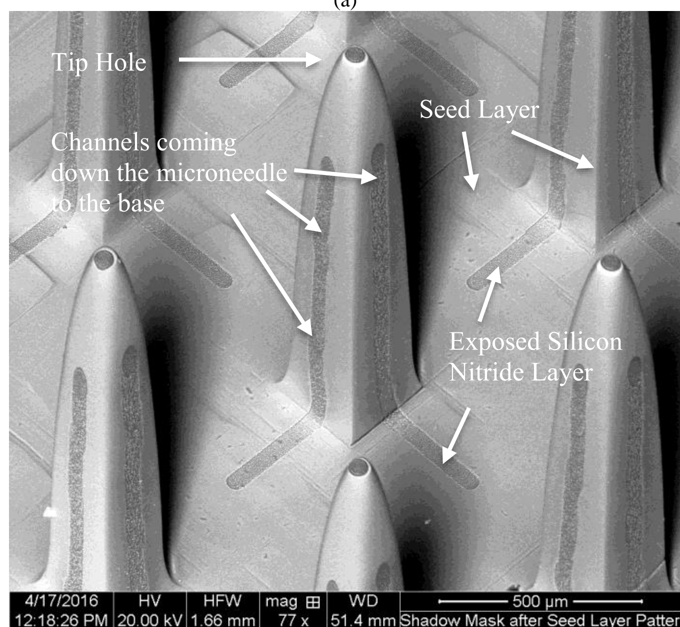

(b)

Figure 6: SEM of seed layer patterning on shadow mask sample: (a) isometric view of full device. (b) zoom in view of couple of patterned microneedles, showing exposed insulation layer.

E. Electroplating

Sample was electroplated in Techni Nickel HT-2 solution, to electrodeposit thicker Ni layer. This makes the structure robust enough to mechanically handle afterwards. Metal grew sidewise in the patterns during electroplating and reduced the pattern width.

For 50 µm trench width

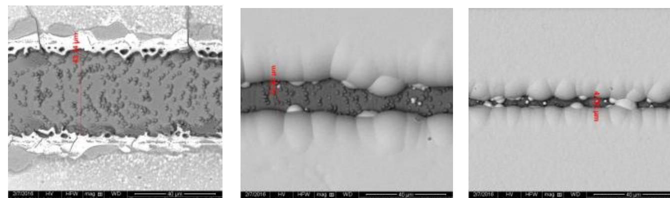

10 mA/Cm^2 **15 mA/Cm^2** **20 mA/Cm^2**

For 30 µm trench width

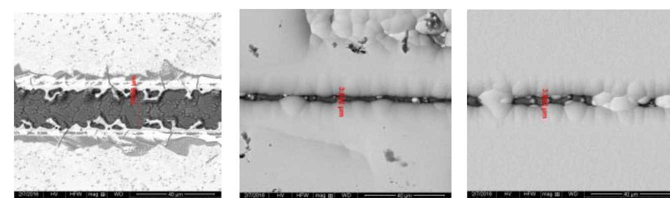

10 mA/Cm^2 **15 mA/Cm^2** **20 mA/Cm^2**

(a)

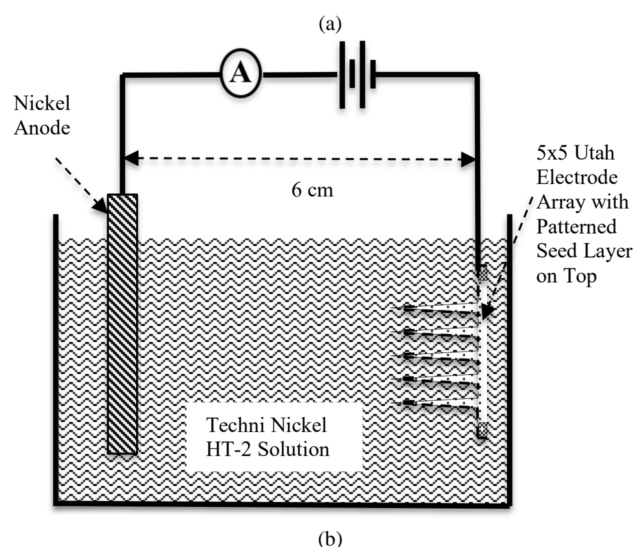

(b)

Figure 7: (a) Electroplating Characterization of sidewise metal growth in laser ablated trenches with different plating current densities: (top three) samples with pre electroplating width of 50 µm, (bottom three) samples with pre electroplating width of 30 µm. (b) Schematic of electroplating setup with Nickel anode and Techni Nickel HT-2 solution. Sample was attached with a conductive wire using silver epoxy (MG Chemicals, Ontario, Canada) and connected with the negative terminal of the voltage source.

Optimum current density for electroplating with Techni Ni HT-2 is between 5 to 22 mA/cm^2. Characterization was carried out to choose appropriate current density to achieve desired pattern width. Laser pattern, using same parameters for pattering on seed layer on microneedle, is used to create patterns with 30 µm and 50 µm initial opening width, on planar sample. Samples were electroplated with three different current densities, shown in figure 7 (a). After plating, opening width was measured. As per the characterization, the pattern

opening can be controlled precisely with current density. Compared to 50 µm pattern width, 30 µm wide patterns showed more probability of getting closed due to sidewise metal growth, as expected.

As pattern width of 35-45 µm was desired, pre electroplating trench width of 50 µm was selected. For that reason, laser spot size of 50 µm was used in the previous step. Current density of 10 mA/cm^2 was used for the electroplating. Figure 7(b) shows the schematic of electroplating setup used in this step. Samples were electroplated for 124 min at 50°C with a Ni anode to get the desired 25 µm thick metal layer. After electroplating, the sample was taken out of the solution and rinsed in DI water. Pattern width was measured from SEM images and found to be 40.84 ± 5.02 µm for the base and for the microneedle it was 39.32 ± 2.98 µm. Thickness was measured to be 26 ± 2 µm.

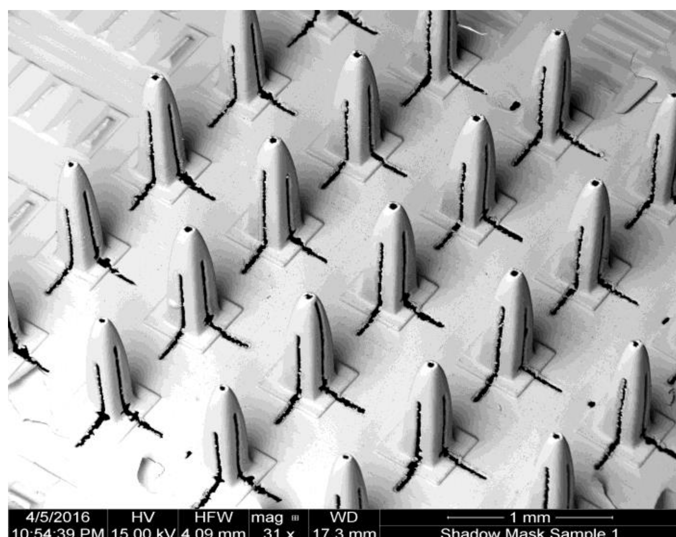

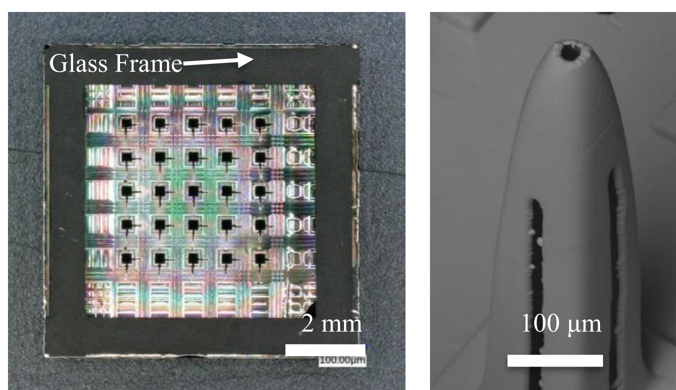

Figure 8: Images of shadow mask sample after etching: (top) SEM of the mask after etching shows the tip holes and patterns along the microneedle towards the base, (bottom left) image on the mask from the backside, showing the hollow microneedles with patterns and glass frame around the mask, (bottom right) zoom in view of one microneedle of shadow mask.

F. Wet Etching

Preferential silicon etchant solution, PSE200, was used at 80°C to remove all the silicon from the sample. After 18 hours of etching the sample was taken out of the solution and rinsed with DI water. Figure 8 shows the shadow mask sample after the wet etching. Images confirmed that all the silicon was etched away and shadow mask was hollow to use as a mask.

IV. Results and Discussion

During the electroplating process, undesired metal growth was observed in the holes. Laser ablation of the seed layer sometimes leave metal particles redeposited in the pattern. This undesired deposition covered a few areas of the patterns. Excimer laser was used again after PSE etching, with higher fluence, to remove the undesired growth. Spot size of 50 µm is used for tip and 40 µm spot was used for the through holes along the microneedle and base with laser fluence of 6239 mj/cm^2 and repetition rate of 200 Hz. For the microneedle,

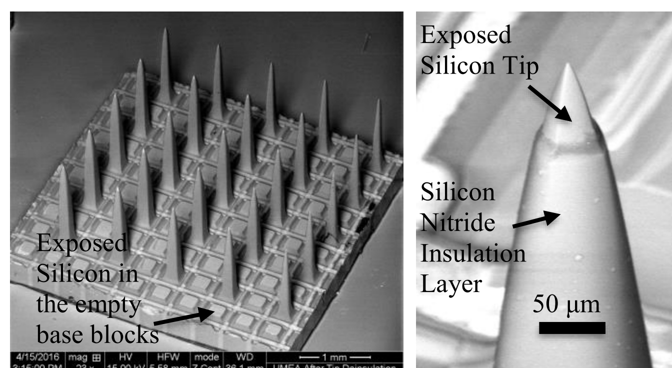

Figure 9: SEM of the UMEA device before metal deposition: (left) 5x5 device with exposed silicon at the tip and base blocks, (right) single microneedle showing insulation layer and exposed silicon tip.

continuous burst of laser was used with a scan speed of 50 µm per second. After every 100 µm pass along the microneedle, focus was readjusted to make sure that sample was in focus.

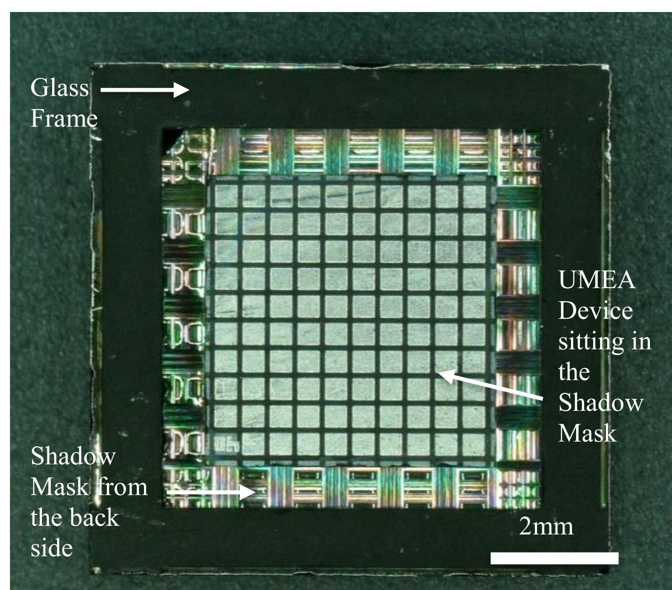

Figure 10: Image of the UMEA device sitting inside a shadow mask.

Ni shadow mask was used on the UMEA device during metal sputtering. The UMEA devices had 50 nm thick atomic

layer deposited Alumina layer and 2 μm thick Silicon Nitride layer on the microneedle as an insulation layer, as illustrated in figure 9. This insulation layer electrically isolates the tip and active sites around the microneedle. The empty base blocks had exposed silicon, where the metal traces electrically connect the active sites on the microneedle to the backside of the bond pad. Silicon at the tip of the microneedle is exposed and has tip exposure of around 50 μm. The fabrication details for UMEA devices are provide in [24].

Shadow mask was placed upside down and UMEA device was placed into the shadow mask, as shown in figure 10. The shadow mask with the device inside was attached on a glass slide using Kapton tape and was placed in the deposition chamber.

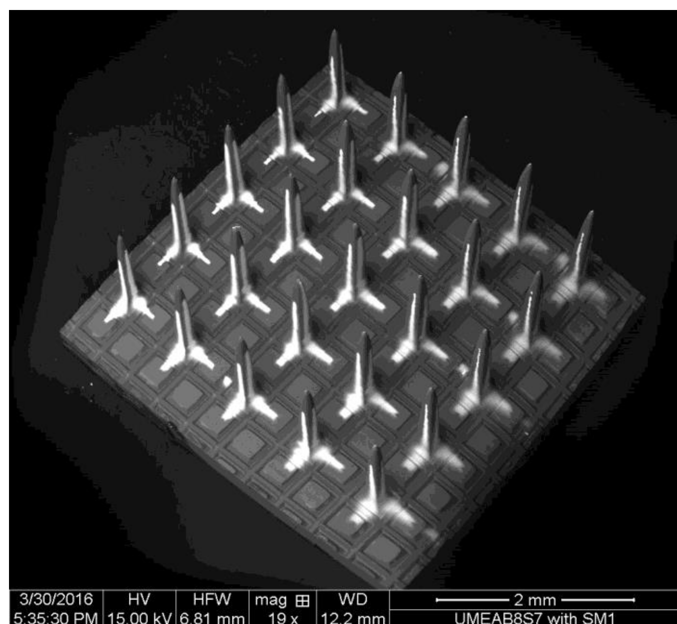

(a)

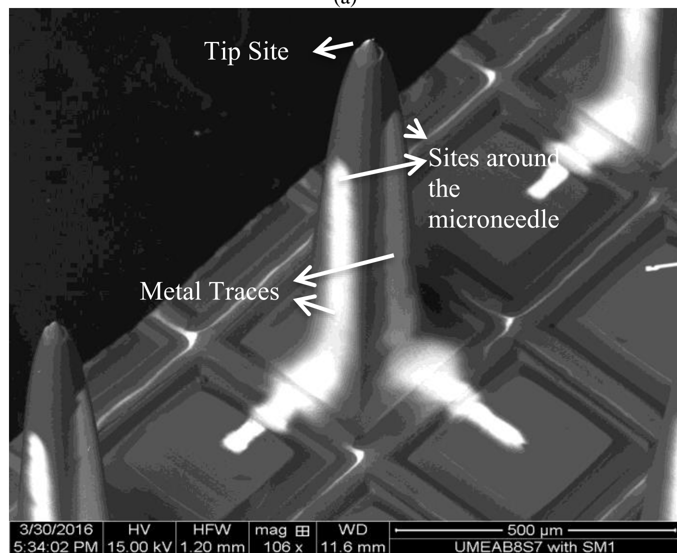

(b)

Figure 11: SEM micrograph of the UMEA device after metal deposition using shadow mask: (**a**) isometric view of the device, (**b**) zoom in view of one microneedle with tip metal site and two metal traces coming down from the microneedle to the base.

We sputtered 40 nm TiW and 900 nm Pt, using TMV Super. TiW was deposited for 4 minutes at a deposition rate of 10 nm per minute, with 20 mTorr of pressure, 45 W of power, and argon gas flow rate of 150 sccm. For Pt, 11 mTorr of pressure, 90 W of power, and argon gas flow of 150 sccm was used to deposit for 45 minutes with a deposition rate of 20 nm per minute. Targets were at angle of 35^0 with the vertical microneedle and 55^0 with the base of the UMEA device. This angled deposition helped the metal particles to go through the patterns and get deposited on the microneedle. To measure the thickness of the metal we used Profilometer (Tencor P-10). The thickness of metal stack was 945 nm.

After the sputtering, xylene was used to remove the adhesive of Kapton tape and shadow mask was taken from the device. UMEA sample was rinsed in N-Butyl alcohol (NBA), IPA and DI water. Figure 11 shows the micrograph of the device after sputtering.

From the micrograph, it is clear that metal went through the patterns in the mask, transferring the patterns onto the 3D microneedle. We got metal at the tip and metal traces running down from the microneedle to the base. Metal traces in the micrographs show different pattern width along the traces. This is primarily due to the difference in gap between the UMEA device and shadow mask. Figure 12 shows the comparison between pattern width on the shadow mask and transferred pattern width on the UMEA device.

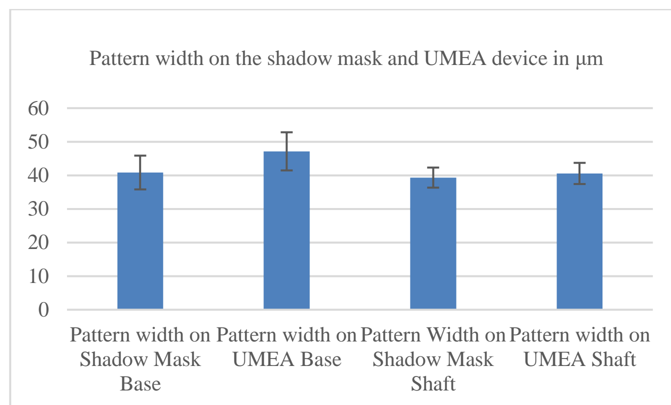

Figure 12: Plot of pattern width on shadow mask and the UMEA device

Pattern opening on the base of the shadow mask was measured to be 40.84 ± 5.02 μm and transferred pattern width on the device was 47.14 ± 5.67 μm. Whereas pattern opening on the shadow mask was 39.32 ± 2.98 μm and transferred pattern width on the device was 40.56 ± 3.15 μm. Blurring effect was seen more on the UMEA base than on the microneedle. This was again due to the distance between shadow mask and the UMEA. A perfect fit of the UMEA to the shadow mask will minimize this blurring.

E-beam evaporation is generally used in vertical metal transfer through shadow mask rather than sputtering [17], as evaporation has higher directionality and hence we can also decrease the blurring effect. The reason we employed sputtering was because of the UEA. The UEA is a food and drug administration (FDA) approved device. Any change in

the process will require time-consuming and expensive tests, as well as optimization for the metal process. We used the same sputtering process parameters to keep the process consistent with present UEA fabrication, but tested for electrical shorts between traces. The traces showed resistance of over 100 MΩ with neighboring traces which indicate no continuity of metal in neighboring trace.

The UMEA device, presented here, has reduced number of recording sites compared to the standard UEA (i.e. UEA has 100 recording sites, whereas the UMEA device has 75 recording sites). Principally, using this approach one can achieve 10x10x3 (300 active sites). However, this would render two-thirds of the sites useless due to unavailability of a connector system for such high channel counts. We used 96 channel connector and hence decided to fabricate 5x5x3 (75) active sites only. New connector will be needed to connect large channel count devices.

The presented method allows the use of laser patterning and electroplating to fabricate shadow mask for patterning high aspect ratio 3D micro devices. Masks can be reused in multiple processing and devices. The fabrication steps can be translated to wafer scale production and also applicable for more complex structures. It is envisioned that Ni shadow mask can be used for etching and ion implantation as well following the works reported in [10].

V. Conclusion

In this paper we presented design, fabrication and application of a high aspect ratio out of plane Ni shadow mask. From the results, it can be concluded that this method of shadow mask fabrication can be useful for complex 3D geometries where standard lithography is not well suited. Furthermore, the shadow mask can be used for MEMS packaging, which requires high aspect ratio patterning. We envision that this method will reduce the process time and variation in pattering on high aspect ratio structure, which will increase the process yield and reduce cost and time as well.

Acknowledgment

This work was performed in part at the Utah Nanofab sponsored by the College of Engineering, Office of the Vice President for Research, and the Utah Science Technology and Research (USTAR) initiative of the State of Utah. The authors appreciate the support of the staff and facilities that made this work possible. This work made use of University of Utah shared facilities of the Micron Technology Foundation Inc. Microscopy Suite sponsored by the College of Engineering, Health Sciences Center, Office of the Vice President for Research, and the Utah Science Technology and Research (USTAR) initiative of the State of Utah.

Disclaimer

Sandeep Negi has financial interest in the company Blackrock Microsystems, which develops and produces implantable neural interfaces, and electrophysiology equipment and software.

References

[1] A. del Campo, and E. Arzt. (2008, Mar.). Fabrication approaches for generating complex micro-and nanopatterns on polymeric surfaces. *Chemical reviews*. [Online]. *108(3)*, pp. 911-945. Available: http://pubs.acs.org/doi/abs/10.1021/cr050018y

[2] P.K. Campbell, K.E. Jones, R.J. Huber, K.W. Horch, and R.A. Normann. (1991, Aug.). A silicon-based, three-dimensional neural interface: manufacturing processes for an intracortical electrode array. *IEEE Trans. on Biomed. Eng.* [Online]. *38(8),* pp. 758-768. Available: http://ieeexplore.ieee.org/stamp/stamp.jsp?tp=&arnumber=83588&isnumber=2726

[3] M.M.H. Shandhi, M. Leber, A. Hogan, R. Bhandari, and S. Negi. (2015, Jun.). A novel method of fabricating high channel density neural array for large neuronal mapping. Presented at Transducers-2015. [Online]. Available: http://ieeexplore.ieee.org/stamp/stamp.jsp?tp=&arnumber=7181286&isnumber=7180834

[4] G.E. Perlin, and K.D. Wise. (2008, Aug.). A compact architecture for three-dimensional neural microelectrode arrays. Presented at *International Conference of the IEEE Engineering in Medicine and Biology Society*. [Online]. Available: http://ieeexplore.ieee.org/document/4650534/?arnumber=4650534&tag=1

[5] F. Barz, T. Holzhammer, O. Paul, and P. Ruther. (2013, Jun.). Novel technology for the in-plane to out-of-plane transfer of multiple interconnection lines in 3D neural probes. Presented at Transducers-2013. [Online]. Available: http://ieeexplore.ieee.org/document/6626909/?arnumber=6626909

[6] M.Y. Cheng, L. Yao, K.L. Tan, R. Lim, P. Li, and W. Chen. (2014, Nov.). 3D probe array integrated with a front-end 100-channel neural recording ASIC. *Journal of Micromechanics and Microengineering*. [Online]. *24(12),* pp. 125010-125021. Available: http://iopscience.iop.org/article/10.1088/0960-1317/24/12/125010/meta

[7] Z. Fekete. (2015, Apr.). Recent advances in silicon-based neural microelectrodes and microsystems: a review. *Sensors and Actuators B: Chemical*. [Online]. *215*, pp. 300-315. Available: http://dx.doi.org/10.1016/j.snb.2015.03.055

[8] F. Barz, O. Paul, and P. Ruther. (2014, Aug.). Modular assembly concept for 3D neural probe prototypes offering high freedom of design and alignment precision. Presented at *International Conference of the IEEE Engineering in Medicine and Biology Society*. [Online]. Available: http://ieeexplore.ieee.org/stamp/stamp.jsp?arnumber=6944495

[9] Y. Choi, S.O. Choi, R.H. Shafer, and M.G. Allen. (2005, Jun.). Highly inclined electrodeposited metal lines using an excimer laser patterning technique. In Presented at Transducers-05. [Online]. Available: http://ieeexplore.ieee.org/stamp/stamp.jsp?tp=&arnumber=1497360&isnumber=32105.

[10] O. Vazquez-Mena, L. Gross, S. Xie, L.G. Villanueva, and J. Brugger. (2015, Jan.). Resistless nanofabrication by stencil lithography: A review. *Microelectronic Eng*. [Online]. *132*, pp. 236-254. Available: http://www.sciencedirect.com/science/article/pii/S0167931714003359

[11] S.Y. Chou, P.R. Krauss, and P.J. Renstrom. (1996, Apr.). Imprint lithography with 25-nanometer resolution. *Science.* [Online]. *272(5258),* pp. 85. Available: http://science.sciencemag.org/content/272/5258/85.

[12] E.C. Alix. (1969, Dec). A convenient stencil for glass etching. *J. Chem. Educ.* [Online]. *46(12)*, pp. 863. Available: http://pubs.acs.org/doi/abs/10.1021/ed046p863.

[13] F.W. Ingle. (1974, Nov.). A shadow mask for sputtered films. *Review of Scientific Inst.* [Online]. *45(11),* pp. 1460-1461. Available: http://scitation.aip.org/content/aip/journal/rsi/45/11/10.1063/1.1686529

[14] L.N. Dunkleberger. (1978, Jan.). Stencil technique for the preparation of thin-film Josephson devices. *Journal of Vac. Sci. & Tech.* [Online]. *15(1),* pp. 88-90. Available: http://scitation.aip.org/content/avs/journal/jvst/15/1/10.1116/1.569443.

[15] H.B. Nguyen. (1980, Jul.). A proposed slotted mask for direct deposition of metal contact pattern on MIS solar cells. *IEEE Trans. on Elect. Dev*. [Online]. *27*, pp. 1303-1304. Available: http://ieeexplore.ieee.org/stamp/stamp.jsp?tp=&arnumber=1480820&isnumber=31804.

[16] G.J. Burger, E.J.T. Smulders, J.W. Berenschot, T.S.J. Lammerink, J.H.J. Fluitman, and S. Imai. (1996, Jun.). High-resolution shadow-mask patterning in deep holes and its application to an electrical wafer feed-through. *Sensors and actuators A: Physical.* [Online]. *54(1-3),* pp. 669-

673. Available: http://www.sciencedirect.com/science/article/pii/S0924424797800350.

[17] J. Brugger, J.W. Berenschot, S. Kuiper, W. Nijdam, B. Otter, and M. Elwenspoek. (2000, Jun.). [Available]. Resistless patterning of sub-micron structures by evaporation through nanostencils. *Microelectronic Eng.* [Online]. *53(1),* pp. 403-405. Available: http://www.sciencedirect.com/science/article/pii/S0167931700003439.

[18] A.R. Champagne, A.J. Couture, F. Kuemmeth, and D.C. Ralph. (2003, Feb.). Nanometer-scale scanning sensors fabricated using stencil lithography. *Applied Physics Letters.* [Online]. *82(7),* pp. 1111-1113. Available: http://scitation.aip.org/content/aip/journal/apl/82/7/10.1063/1.1554483

[19] J. Brugger, C. Andreoli, M. Despont, U. Drechsler, H. Rothuizen, and P. Vettiger. (1999, Aug.). Self-aligned 3D shadow mask technique for patterning deeply recessed surfaces of micro-electro-mechanical systems devices. *Sensors and Actuators A: Physical.* [Online]. *76(1),* pp. 329-334. Available: http://www.sciencedirect.com/science/article/pii/S0924424798002866

[20] G. Villanueva, O. Vazquez-Mena, C. Hibert, and J. Brugger. (2009, January). Direct etching of high aspect ratio structures through a stencil. Presented at MEMS-2009. [Online]. Available: http://ieeexplore.ieee.org/stamp/stamp.jsp?tp=&arnumber=4805339&isnumber=4805295.

[21] G.H. Kang, K.Y. No, and G.M. Kim. (2006, Oct.). Fabrication of microchannel with electrodes on side wall. Int. *Journal of Modern Physics B.* [Online]. *20(25n27),* pp. 4493-4498. Available: http://www.worldscientific.com/doi/abs/10.1142/S0217979206041574.

[22] S.O. Choi, S. Rajaraman, Y.K. Yoon, X. Wu, and M.G. Allen. (2006). 3-D patterned microstructures using inclined UV exposure and metal transfer micromolding. Presented at Proc. Solid State Sensors, Actuators and Microsystems Workshop (Hilton Head, SC). [Online]. Available: http://citeseerx.ist.psu.edu/viewdoc/download?doi=10.1.1.561.4571&rep=rep1&type=pdf.

[23] J.H. Choi, and G.M. Kim. (2011, Feb). Micro-patterning on non-planar surface using flexible microstencil. *International Journal of Precision Engineering and Manufacturing.* [Online]. 12(1), pp. 165-168. Available: http://link.springer.com/article/10.1007/s12541-011-0023-x.

[24] M.M.H. Shandhi, M. Leber, A. Hogan, D.J. Warren, R. Bhandari, and S. Negi, "Fabrication of high channel density neural array for cortical stimulation," unpublished.

Md. Mobashir Hasan Shandhi received the BSc degree in Electrical and Electronics Engineering from Bangladesh University of Engineering & Technology (BUET), Dhaka, Bangladesh, in 2011 and the MSc degree in Electrical and Computer Engineering (ECE) from University of Utah, Salt Lake City, Utah, USA, in 2016. From 2011 to 2014, he was a lecturer in American International University – Bangladesh (AIUB), Dhaka, Bangladesh. He is currently pursuing his Ph.D. degree in ECE at Georgia Institute of Technology. His research interests include bioMEMS, wearable biosensors and home monitoring devices.

Moritz Leber received the German Dipl.-Ing. (M.Sc.) degree from Saarland University, Saarbrücken, Germany, in 2014, and the French Diplôme d'Ingénieur (M.Sc.) degree from the École Nationale Supérieure d'Ingénieurs en Informatique Automatique Mécanique Énergétique Électronique (ENSIAME), Valenciennes, France, in 2014. During his studies at Saarland University, he worked at the lab for measurement technology LMT (2009 - 2010) and at the lab for micromechanics, microfluidics/microactuators LMM (2013 - 2014), as well as at the lab for nondestructive testing and quality assurance in cooperation with the Fraunhofer Institute for nondestructive testing IZFP (2012 - 2013), Saarbrücken, Germany.

In 2014, he joined the department of electrical and computer engineering at the University of Utah, where he is currently enrolled as Ph.D. student. His research interests include measurement and sensor technology, micro-systems, micro-fabrication, and micro-electrodes for neural interfaces.

Alexander L. Hogan received the B.S. degree and the M.S. degree both in electrical engineering from the University of Utah, Salt Lake City, UT, USA, in 2011 and 2012 respectively. From 2007 to 2013 he was with the University of Utah Nanofab, Salt Lake City, UT, USA. During the summer of 2010 he completed an internship at Sandia National Laboratory. He is currently a R&D Array Engineer at Blackrock Microsystems, Salt Lake City, UT, USA. His research covers microsystems design, fabrication and application and is currently focused on implantable neural interfaces.

David J. Warren (M'76- SM'14) received the B.S. degree in electrical engineering from Washington State University, Pullman, in 1979; the M.S. degree in electrical engineering from the University of Washington, Seattle, in 1982; and the Ph.D. degree in bioengineering from the University of Utah, Salt Lake City in 2006.

Currently, he is a Research Assistant Professor in the Department of Bioengineering, University of Utah. His research focuses on the decoding of afferent and encoding of efferent neuronal signals in the peripheral nervous system to restore sensory and motor function after spinal cord injury or limb loss.

Rajmohan Bhandari received MS degrees in Physics from Garhwal University, Dehradun, India in 1996. In 2000 he received MTech degree from Physics department from Indian Institute of Technology (IIT), Delhi, India, with majors in MEMS. In 2009 in US he received his PhD degree in Electrical and Computer Engineering from University of Utah. He worked in MEMS company in Singapore, as a product engineer, from 2001 to 2004. Since 2008, he is with Blackrock Microsystems and currently, he is the Director of array business. His research interests include neural prosthesis, BioMEMS, biocompatible materials, and system integration.

Sandeep Negi received the BS and MS degrees in physics from Garhwal University, Dehradun, India, in 1996 and 1998, and the MTech degree in physics from Indian Institute of Technology (IIT), Delhi, India, in 2000. He received the PhD degree in 2009 in electrical and computer engineering from University of Utah, Salt Lake City, USA. From 2001 through 2004, he worked in MEMS industry in Singapore. From 2004 through 2005, he worked as research assistant in University of Calgary, Calgary, Alberta, Canada. From 2009 to 2012 and then 2015 till date he is with a leading biomedical company in Salt Lake City, USA. From 2012 to 2015, he was faculty electrical and computer engineering from University of Utah, Salt Lake City, USA. His research interest includes biomaterials and BioMEMS devices especially for neural prosthesis.